HHS Public Access

Author manuscript

*Development*. Author manuscript; available in PMC 2018 March 14.

Published in final edited form as:

*Development*. 2006 December ; 133(24): 4945–4955. doi:10.1242/dev.02694.

# T-Box transcription factor Tbx20 regulates a genetic program for cranial motor neuron cell body migration

**Mi-Ryoung Song**[1], **Ryuichi Shirasaki**[1,*], **Chen-Leng Cai**[2], **Esmeralda C. Ruiz**[1,†], **Sylvia M. Evans**[2], **Soo-Kyung Lee**[1,‡], and **Samuel L. Pfaff**[1,§]

[1]Gene Expression Laboratory, The Salk Institute, La Jolla, CA 92037, USA

[2]Department of Medicine, University of California, San Diego, 9500 Gilman Drive, La Jolla, CA 92093, USA

## Abstract

Members of the T-box transcription factor family (Tbx) are associated with several human syndromes during embryogenesis. Nevertheless, their functions within the developing CNS remain poorly characterized. *Tbx20* is expressed by migrating branchiomotor/visceromotor (BM/VM) neurons within the hindbrain during neuronal circuit formation. We examined Tbx20 function in BM/VM cells using conditional *Tbx20*-null mutant mice to delete the gene in neurons. Hindbrain rhombomere patterning and the initial generation of post-mitotic BM/VM neurons were normal in *Tbx20* mutants. However, Tbx20 was required for the tangential (caudal) migration of facial neurons, the lateral migration of trigeminal cells and the trans-median movement of vestibuloacoustic neurons. Facial cell soma migration defects were associated with the coordinate downregulation of multiple components of the planar cell polarity pathway including Fzd7, Wnt11, Prickle1, Vang1 and Vang2. Our study suggests that Tbx20 programs a variety of hindbrain motor neurons for migration, independent of directionality, and in facial neurons is a positive regulator of the non-canonical Wnt signaling pathway.

### Keywords

Tbx20; Migration; Branchiomotor; Hindbrain; Wnt; Planar cell polarity; Mouse

## INTRODUCTION

Cell migration is a crucial feature of organogenesis and tissue formation during embryogenesis. Likewise, in the developing brain, many classes of newly formed neurons migrate in stereotypic patterns in order to establish the proper cytoarchitecture of the

[§]Author for correspondence (pfaff@salk.edu).

[*]Present address: Cellular and Molecular Neurobiology Laboratory, Graduate School of Frontier Biosciences, Osaka University, Suita, Osaka 565-0871, Japan

[†]Present address: Biomedical Sciences Graduate Program, University of California, San Diego, 9500 Gilman Drive, La Jolla, CA 92093, USA

[‡]Present address: Department of Molecular and Cellular Biology, Huffington Center on Aging, Baylor College of Medicine, Houston, TX 77030, USA

**Supplementary material**

Supplementary material for this article is available at http://dev.biologists.org/cgi/content/full/133/24/4945/DC1

nervous system (Hatten, 1999; Marin and Rubenstein, 2003). Neuronal migration increases the cellular complexity within each region of the brain and presumably facilitates the assembly of more complex circuits. Members of the T-box transcription factor family (Tbx) have been linked to the proper development of migrating cells (reviewed by Naiche et al., 2005; Smith, 1999). During gastrulation, brachyury and Tbx2b control the cellular reorganization of the embryo that drives convergent extension and notochord formation (Fong et al., 2005; Wilkinson et al., 1990). Similarly, Tbx5 and Tbx20 have been implicated in the cardiac cell migration associated with the formation of heart chambers (Cai et al., 2005; Hatcher et al., 2004; Singh et al., 2005; Stennard et al., 2003; Stennard et al., 2005), Tbx1 in neural crest migration and proper middle/inner ear development (Moraes et al., 2005), and Tbr1 in cellular organization within the cerebellum (Fink et al., 2006).

Tbx20 is expressed by migratory branchiomotor (BM) and visceromotor (VM) neurons in the hindbrain (Ahn et al., 2000; Kraus et al., 2001). BM neurons innervate branchial arch-derived muscles that control jaw and eye movement, facial expression, and muscles within the pharynx and larynx. VM cells innervate parasympathetic ganglia to control lacrimal gland activity and salivation. During hindbrain development, trigeminal (V) BM cell bodies migrate dorsolaterally within rhombomeres 2-3 (r2-3) (summarized in Fig. 1I-L). Facial (VII) VM cells move dorsolaterally and settle in a unique location near the pial surface of r5, whereas the BM component of the facial nucleus is generated within r4 but moves tangentially along the anteroposterior axis of the hindbrain into r6 and then migrates dorsolaterally. Interestingly, vestibuloacoustic (VIII) neurons, which provide efferent input to the inner ear, are also generated within r4 and exhibit a very unique migratory pattern in which their cell bodies cross the midline to the contralateral side of the hindbrain (Fritzsch, 1996; Simon and Lumsden, 1993; Tiveron et al., 2003). Thus, multiple subclasses of motor neurons are generated in specific locations within the hindbrain. Although each of these motor neuron subtypes displays a unique pattern of cell migration, all of them are apparently related by virtue of expressing Tbx20. Nevertheless, the function of Tbx20 in these distinct populations of migratory cells is unknown.

Several observations indicate that facial neurons are responsive to extrinsic cues within their local environment. In *Kreisler* (*Mafb* – Mouse Genome Informatics) and *Krox20* (*Egr2* – Mouse Genome Informatics) mutant mice, r5 progenitors acquire an r6-like identity (Manzanares et al., 1999; Schneider-Maunoury et al., 1993; Seitanidou et al., 1997; Swiatek and Gridley, 1993). Despite their re-specification, facial cells initiate their typical pattern of caudal migration but prematurely move radially once they encounter the new environment adjacent to r4 (Garel et al., 2000; Schneider-Maunoury et al., 1997). Although these studies demonstrate that r5 is not required to initiate tangential migration, transplants of mouse r5 tissue placed homotopically into chick embryos trigger ectopic facial cell migration (Studer, 2001). Vascular endothelial growth factor (*VEGF164*) mutant mice exhibit tangential migration defects of facial motor neurons indicating that this factor may selectively attract facial BM cells (Schwarz et al., 2004).

The intrinsic factors controlling facial motor neuron migration have begun to emerge through extensive genetic studies. A transcriptional cascade including Hoxb1, Gata2, Gata3 and Phox2b regulates their identity and migration (Bell et al., 1999b; Goddard et al., 1996;

Nardelli et al., 1999; Pata et al., 1999; Pattyn et al., 2000; Studer et al., 1996). Transcription factors expressed at later stages, such as Nkx6.1 (Nkx6-1 – Mouse Genome Informatics) and Ebf1, are dispensable for facial motor neuron specification but are necessary for their tangential migration (Garel et al., 2000; Muller et al., 2003). Cell surface molecules and intracellular signaling components have been implicated in facial neuron migration. Mouse mutants of the VEGF164 receptor gene neuropilin 1 exhibit tangential migration defects comparable to *VEGF164* mutants (Schwarz et al., 2004). Zebrafish mutants *trilobite* and *strabismus* (*vang-like 2* – Zebrafish Information Network), *van gogh* (*vang-like 1* – Zebrafish Information Network) and *prickle1* (*pk1*), which are components of the planar cell polarity pathway (PCP), arrest facial neuron migration (Bingham et al., 2002; Carreira-Barbosa et al., 2003; Jessen et al., 2002). Nevertheless, the relationship between facial cell migration and that of the other hindbrain motor neuron classes is not well understood, and it is unclear whether shared gene regulatory networks are used for the migration of distinct motor neuron subtypes.

Here, we show that *Tbx20* is selectively expressed by divergent classes of migratory motor neurons within the hindbrain. The regional patterning of the rhombomeres and generation of post-mitotic motor neurons were normal in *Tbx20* conditional mutants, consistent with the relatively late but selective onset of Tbx20 expression in post-mitotic BM/VM neurons. *Tbx20* mutants displayed an assortment of cell migration defects including abnormal dorsolateral migration of BM trigeminal cells and VM facial neurons, arrested tangential migration of facial BM neurons, and a lack of trans-median migration of vestibuloacoustic cells. We found that hindbrain motor neurons lacking *Tbx20* retained the ability to extend neurites into the periphery; thus, it is unlikely that the severe disruption of neuronal migration in these mutants arises indirectly from a loss of axons that might provide a substrate for soma translocation. Deletion of *Tbx20* resulted in the downregulation of *Tbx2* and key components of the PCP pathway. Together, our results demonstrate that Tbx20 is shared by a variety of BM/VM neurons to regulate their proper cell body migration.

## MATERIALS AND METHODS

### Mouse lines

The generation of *Tbx20*-null and *Tbx20* floxed mice and of transgenic mouse line *SE1::gfp* have been reported previously (Cai et al., 2005; Shirasaki et al., 2006). Neural-specific *Tbx20* conditional mutant mice were obtained by crosses between a heterozygous animal carrying a null allele of *Tbx20* and a *Nestin::Cre* allele (Jackson Laboratory), and a homozygous animal carrying a $Tbx20^{fl}$ conditional allele, to produce animals with the genotype: $Tbx20^{fl/KO}$; $Nestin::Cre^{+/-}$. *Ret* mutant mice have been described previously (Schuchardt et al., 1994) and were kindly provided by F. Costantini (Columbia University, New York, USA).

### Immunohistochemistry

Embryos were obtained and processed for immunohistochemistry as previously described (Thaler et al., 1999). To generate a Tbx20-specific antibody, a peptide corresponding to amino acids 426-445 of mouse Tbx20 was synthesized, coupled to hapten and injected into

rabbits. Additional antibodies used in this study are: guinea pig anti-Isl1 (Thaler et al., 2004), rabbit anti-Isl1/2 (Ericson et al., 1992), rabbit anti-Phox2b (Pattyn et al., 2000), rabbit and guinea pig anti-Hb9 (Thaler et al., 1999), rabbit anti-Lhx3 (Sharma et al., 1998), rabbit anti-GFP (Invitrogen), monoclonal anti-HA (Babco), monoclonal anti-MNR2 (Developmental Studies Hybridoma Bank) (Tanabe et al., 1998), rabbit anti-Nkx6.1 (Beta Cell Biology Consortium) and goat anti-GATA2 (Santa Cruz) antibodies. Fluorophore-conjugated species-specific secondary antibodies were used as recommended (Jackson Laboratory and Invitrogen). For whole-mount neurofilament staining, embryos were fixed, permeabilized with a graded methanol series and incubated with rabbit anti-neurofilament antibody (Chemicon) followed by HRP-conjugated secondary antibody (Jackson Laboratory) for DAB staining.

### In situ hybridization

Embryos were fixed in 4% paraformaldehyde, mounted and cryosectioned for in situ hybridization. Transverse sections were hybridized with digoxigenin-labeled probes specific for individual genes. Each cDNA sequence used to generate probes was amplified from mouse or chick embryonic cDNA using the Advantage cDNA PCR Kit (Clontech) and TOPO Cloning Kit (Invitrogen). For flat-mounted hindbrain in situ hybridization, hindbrains were dissected and processed as previously described with minor modification (Garel et al., 2000; Ohsawa et al., 2005). Briefly, dissected hindbrains were fixed, permeabilized with methanol and proteinase K treatment, hybridized with digoxigenin-labeled probes, incubated with anti-digoxigenin alkaline phosphatase-conjugated antibody (Roche), and developed with NCIP/NBT substrates (Roche). Specimens were cleared with glycerol and flat-mounted for visualization.

### Flat-mount hindbrain culture

Embryonic day (E) 11.5 mouse embryos were used. Flat-mounted preparations of the hindbrain were prepared as previously described (Shirasaki et al., 1995). The neural tube of the hindbrain region was dissected, cut along the dorsal midline and flat-mounted in ice-cold DMEM/F12 (Invitrogen). The hindbrain was then placed on a collagen-coated membrane in a 6-well tissue culture plate (Yamamoto et al., 1989) (Transwell Collagen, Corning Costar) with the ventricular side facing down, and cultured in the medium for 30 hours as described (Shirasaki et al., 1998). After culture, the preparations were fixed in 4% paraformaldehyde in PB for 2 hours at room temperature, followed by several rounds of washing with PBS. The preparations were then detached from the membrane filter and immunohistochemistry was performed as described above.

### Chick in ovo electroporation

Chick eggs (Charles River and McIntyre Farms) were incubated in a humidified chamber. DNA constructs were injected into the lumens of chick embryonic spinal cords at HH stage 10 to 12. Electroporation was performed using a square wave electroporator (BTX) (Nakamura et al., 2000). Coelectroporation resulted in >80% of cells expressing all constructs. Incubated chicks were harvested and analyzed at HH stage 20 to 25.

# RESULTS

## Tbx20 is expressed in multiple classes of branchiomotor and visceromotor neurons

To investigate the role of Tbx20 in neuronal development, we defined its expression pattern in mouse embryos using in situ hybridization. *Tbx20* expression was first detected at E10.5 in two stripes of cells extending the length of the hindbrain, corresponding to the location of developing motor neurons (Fig. 1A) (Kraus et al., 2001). The pattern of *Tbx20* expression was similar to that of transcription factors Isl1 and Phox2b, whose overlapping expression marks BM/VM neurons (Fig. 1E) (Pata et al., 1999; Pattyn et al., 2000). As development progressed from E10.5 to E13.5, the location of *Tbx20*$^{+}$ cells closely matched the position of migrating Isl1$^{+}$/Phox2b$^{+}$ BM/VM neurons along the entire anteroposterior axis of the hindbrain (Fig. 1A-H).

Next, we generated an antibody against a unique peptide sequence at the carboxy terminal end of the protein and performed immunocytochemistry. From the onset of expression at E10.5, Tbx20 was restricted to Isl1$^{+}$ motor neurons (see Fig. S1 in the supplementary material). Medially-located cells emerging from the ventricular zone expressed Isl1 but not Tbx20 (Fig. 1M, and see Fig. S1 in the supplementary material), suggesting that Tbx20 expression occurs shortly after Isl1. Since Isl1 expression is closely associated with the post-mitotic birth of motor neurons (Ericson et al., 1992), Tbx20 expression is likely to be initiated after neuroepithelial cells have exited the cell cycle. The location of the Isl1$^{+}$/Tbx20$^{+}$ cells corresponded to the position of facial BM neurons (VII) in r4 (Fig. 1M). However, Tbx20 was not detected in the somatic motor (SM) population of abducens (VI) motor neurons (Fig. 1P, and see Fig. S1 in the supplementary material), although it was found in the adjacent facial BM neurons at r5. Similarly, SM hypoglossal (XII) neurons did not express Tbx20, whereas the adjacent vagal (X)/cranial accessory (XI) BM neurons were labeled at r8 (see Fig. S1 in the supplementary material). Vestibuloacoustic (VIII) neurons are generated together with facial cells in r4 and express Gata2 and Gata3 which distinguishes them from the facial population which downregulate these factors upon differentiation (Bell et al., 1999a; Tiveron et al., 2003). At E11.5, Tbx20 was detected in the ventral Gata2$^{+}$/Isl1$^{+}$ vestibuloacoustic cells (Fig. 1M-O). Based on these labeling patterns, we conclude that trigeminal (V), facial (VII), vestibuloacoustic (VIII), glossopharyngeal (IX), vagal (X) and spinal accessory (XI) motor neuron groups express Tbx20 (Fig. 1I-L). Thus, the dorsal-settling cranial motor neurons comprising the BM/VM cell groups express Tbx20 during their cell migration period, whereas ventral-settling SM cells within the abducens (VI) and hypoglossal (XII) nuclei lack this T-box factor.

## Motor neuron specification is normal in the absence of Tbx20

*Tbx20* mutant mouse embryos die at around E10.5 due to cardiac defects prior to the main period of hindbrain motor neuron development (Cai et al., 2005; Singh et al., 2005; Stennard et al., 2005). We thus generated conditional *Tbx20* mutant mice selectively lacking Tbx20 expression in neurons (Cai et al., 2005). *Tbx20*$^{fl/fl}$ mice were mated to *Tbx20*$^{ko/wt}$; *Nestin::Cre* animals. Embryos with the genotype *Tbx20*$^{fl/ko}$; *Nestin::Cre* (abbreviated to *Tbx20* cKO) were used for our analysis. This genetic strategy was chosen because nestin is broadly expressed in neuronal progenitor cells and only one allele of *Tbx20* required

recombination to generate *Tbx20*-null cells. *Tbx20* cKO embryos lacked Tbx20 protein expression from the outset of motor neuron development in the hindbrain (Fig. 2A,B, and see Fig. S2 in the supplementary material). In situ hybridization using exon 2-specific probes demonstrated that this segment had been deleted as expected (see Fig. S2 in the supplementary material). These findings indicate that the recombination of $Tbx20^{fl}$ is efficient and occurs prior to the normal expression of Tbx20 in motor neurons. The development of *Tbx20* cKO embryos appeared to be normal up to E12.0. After E12.5, however, *Tbx20* mutants began to die due to apparent heart defects caused by transient expression of *Nestin::Cre* in developing cardiac cells. Thus, we focused our analysis of hindbrain development on stages from E10.5-E12.0.

We first examined whether the absence of Tbx20 prevented the specification of BM/VM neurons, focusing on the r4 level of the hindbrain. The truncated Δ*Tbx20* transcript remaining in the conditional mutants was used as a lineage marker to identify *Tbx20*-null cells. We found that the motor neurons normally destined to express Tbx20 were still present in E11.5 *Tbx20* cKO embryos (Fig. 2C,D). At the r4 level, a detailed genetic cascade has been defined for facial and vestibuloacoustic neuron specification. Hoxb1 is thought to confer rhombomere 4 cell identity, leading to the subsequent activation of Mash1 and Math3 (Ascl1 and Neurod4, respectively – Mouse Genome Informatics), Gata2, Phox2b, Isl1 and Nkx6.1 (Muller et al., 2003; Ohsawa et al., 2005; Pata et al., 1999; Pattyn et al., 2000). Transverse sections taken at r4 of E11.5 *Tbx20* cKO embryos revealed a normal distribution of *Hoxb1*, *Math3* and *Mash1* expression in progenitor cells and newly formed motor neurons (Fig. 2E-J). Furthermore, the detection of $Nkx6.1^{+}/Isl1^{+}$ post-mitotic motor neurons suggested that the initial specification of these cells was unaffected in *Tbx20* cKO embryos (Fig. 2K,L). Likewise, Phox2a, whose expression is restricted to post-mitotic facial cells, was present in r4 from *Tbx20* cKO embryos (Fig. 2M,N). Similarly, the general pattern of *Gata2* labeling was essentially unchanged in flat-mounted hindbrains from *Tbx20* mutants, although the medial nVIII cells within r4 failed to express *Gata2* when *Tbx20* was deleted (Fig. 2O,P, and data not shown). Although many features of hindbrain development appeared normal in *Tbx20* cKO embryos, we found that the anteroposterior distribution of facial BM neurons marked by Phox2b was altered in the mutants (Fig. 2Q,R). Taken together, these findings indicate that the elimination of *Tbx20* from r4-derived facial motor neurons does not disrupt their specification nor initial generation, but does appear to hinder the tangential migration of their cell bodies.

The expression of Tbx20 in BM/VM cells, but not in SM neurons, raised the possibility that a conversion in motor neuron identity may have occurred in *Tbx20* cKO embryos. Since SM neurons migrate along different pathways, this could in principle account for the facial neuron migration defect. A conversion of BM/VM cells to SM neurons should be accompanied by an altered gene expression profile. To test this we examined whether Hb9 (Hlxb9 – Mouse Genome Informatics), a marker for SM cells, had become ectopically activated in cells normally fated for a BM/VM identity. As expected, Hb9 was expressed normally in SM neurons forming the abducens (r5) and hypoglossal (r8) cell populations in *Tbx20* cKO embryos (Fig. 3A,B). Importantly, regions of the hindbrain, such as r4, that lack SM neurons did not ectopically express Hb9 in the conditional mutants, arguing against the possibility of cell fate conversion. Next, we examined the hindbrain at E10.5, which

precedes the main period of cell migration. The distribution of Isl1$^+$/Phox2b$^-$ SM neurons and Isl1$^+$/Phox2b$^+$ BM neurons at r8 was similar in the *Tbx20* cKO mutants and controls (Fig. 3C,D). Likewise, the number of Hb9$^+$ cells at r5 and r8 levels of the hindbrain were unchanged in *Tbx20* cKO embryos (Fig. 3E). These results suggest that the elimination of Tbx20 does not cause a wholesale switch of BM/VM cells to SM neurons.

## Motor neuron soma migration is disrupted in *Tbx20* mutants

Although BM/VM neurons appeared to be specified properly based on their expression of marker genes, we found that the cells became ectopically located in *Tbx20* cKO mutants. In control embryos at E11.5, Isl1$^+$ facial BM neurons have begun to migrate caudally past the Hb9$^+$ abducens cells generated at r5 (Fig. 4A). Facial neurons failed to migrate caudally in *Tbx20* mutants (Fig. 4B). The dorsolateral migration of trigeminal neurons was also disrupted in *Tbx20* mutants (Fig. 4A,B). Normally, trigeminal cells at r2-3 have migrated dorsolaterally by E11.5 (Fig. 4A), but in *Tbx20* mutants the cells were still visible adjacent to the midline (Fig. 4B). A day later in development, at E12.5, trigeminal cells were found scattered along the mediolateral axis of *Tbx20* mutants, stalled in their laterally-directed migration (see Fig. 5C,D,G,H). These results were further confirmed by examining the distribution of Phox2b$^+$/Isl1$^+$ trigeminal neurons in transverse sections taken at specific rhombomere levels. By E11.5, the majority of trigeminal neurons had migrated into the lateral half of r2-3 in control embryos, whereas most of the Phox2b$^+$/Isl1$^+$ cells were located medially in *Tbx20* conditional mutants (Fig. 4C,D,I). Similarly, at r4 levels, the lateral migration of the VM subclass of facial neurons initiated their lateral migration but failed to reach their final destination (Fig. 4E,F). Furthermore, the caudal migration of facial BM neurons resulted in a large number of Phox2b$^+$/Isl1$^+$ cells entering r6 in control embryos, whereas no facial neurons were observed in r6 E11.5 *Tbx20* mutants (Fig. 4G,H,J).

Next we sought to determine whether the trans-median migration of vestibuloacoustic cells across the r4 midline requires Tbx20. To visualize vestibuloacoustic motor neurons we crossed the *SE1::gfp* transgene reporter into the *Tbx20* conditional mutant background. *SE1::gfp* transgenic mice express GFP under the control of an Isl1 enhancer active in cranial motor neurons (see Fig. S3 in the supplementary material) (Shirasaki et al., 2006; Uemura et al., 2005). The reporter mice revealed migrating vestibuloacoustic cell bodies and their axonal processes within the rhombomere 4 midline (Fig. 4K). The absence of GFP labeling in the r4 midline indicated that vestibuloacoustic neurons failed to migrate to the contralateral side of the hindbrain in *Tbx20* mutants (Fig. 4L). Thus, our results indicate that multiple types of migration defects arise in *Tbx20* mutants: (1) the dorsolateral migration of trigeminal and facial VM cells is disrupted; (2) the caudal (tangential) migration of facial BM neurons is blocked; and (3) the trans-median migration of vestibuloacoustic neurons is defective (Fig. 4M,N).

## *Tbx20* mutants display subtle defects in peripheral motor axon projections

Migration defects in BM/VM neurons in the absence of Tbx20 prompted us to examine whether axons of these cells innervate their peripheral targets normally. To examine the axon projections of trigeminal and facial neurons, we used the *SE1::gfp* line to selectively label the cells. Despite the abnormal cell body settling of trigeminal and facial neurons in *Tbx20*

mutants, we found that their axons selected the correct exit points from r2 and r4, respectively (Fig. 5A-H). Next we labeled the peripheral projections of cranial neurons by performing neurofilament staining on E11.5 embryos. The overall pathfinding of both trigeminal and facial neurons appeared normal (Fig. 5I,L). However, the axon terminals of facial neurons were not normal in *Tbx20* mutants. The distal ends of wild-type facial motor axons exhibit a characteristic triangular pattern at this stage, whereas facial neurons in *Tbx20* mutants extended axons beyond their normal stopping point and occasionally were misrouted and looped back (Fig. 5J,M). Similarly, subtle defects in the routing and fasciculation of vagal axons were noted in *Tbx20* mutants (Fig. 5K,N). These data confirm that the overall ability of BM/VM neurons to properly extend axons into the periphery is preserved in *Tbx20* mutants, but that subtle axon pathfinding errors exist.

## Cell body migration defects in *Tbx20* mutants are not due to developmental arrest

In principle, the soma migration defects in *Tbx20* mutants could arise because embryos develop more slowly. To exclude this possibility and establish that migration defects are autonomous to the neuroepithelial cells, we used organotypic culture of the hindbrain to extend the survival of the mutant tissue. Hindbrains from *SE1::gfp* transgenic mice were dissected from E11.5 embryos and cultured as flat-mounts. GFP and Isl1 labeling were used to monitor the cell body position of motor neurons after culturing for 30 hours. During the culture period we found a marked increase in the number of $Isl1^{+}/GFP^{+}$ motor neurons that migrated caudally from r4 into r5/6 (Fig. 6A-D). Facial BM neurons within hindbrains derived from *Tbx20* mutant embryos failed to migrate caudally after 30 hours, in contrast to the migration observed with controls (Fig. 6E,F). Likewise, the dorsolateral migration of trigeminal neurons also failed to occur in explants derived from *Tbx20* mutants, whereas trigeminal cell migration was observed with controls (Fig. 6G,H). These findings indicate that the lack of BM/VM neuron migration observed in *Tbx20* mutants is unlikely to be due to a general delay in the development of these embryos.

## Gene expression profile is altered in *Tbx20* mutants

Tbx20 has been found to directly repress the expression of Tbx2 in myocardial cells within the developing heart (Cai et al., 2005; Singh et al., 2005; Stennard et al., 2005). To determine whether similar genetic interactions operate within hindbrain motor neurons, we examined the expression of *Tbx2* in *Tbx20* mutants using in situ hybridization. Unlike in the heart, Tbx2 and Tbx20 are co-expressed by BM/VM neurons rather than being mutually exclusive (Fig. 7A). *Tbx2* mRNA levels were significantly reduced in trigeminal cells (V) and almost undetectable in facial BM neurons (VII) from *Tbx20* mutants (Fig. 7A-F). Thus, Tbx20 appears to activate Tbx2 expression in motor neurons and repress it in myocardial cells. Similarly, Tbx20 represses Isl1 in myocardial cells (Cai et al., 2005), whereas Isl1 and Tbx20 are co-expressed in cranial motor neurons (see Fig. 1M). Furthermore, Isl1 is not upregulated in cranial motor neurons in *Tbx20* mutants (Fig. 4A,B, Fig. 8Y). To examine the genetic interaction among transcription factors defining BM neurons, we ectopically expressed Phox2a in the chick embryonic neural tube using in ovo electroporation. Previous studies have shown that the closely related Phox2b transcription factor is sufficient to trigger ectopic BM/VM neuron differentiation (Dubreuil et al., 2000). We found that Phox2a induced the ectopic expression of the motor neuron marker Isl1 within the dorsal neural tube

(Fig. 7G). Adjacent sections revealed that the Isl1$^+$ cells also expressed *Tbx20* and *Tbx2* (Fig. 7G-I). However, misexpression of Tbx20 failed to induce Tbx2 (data not shown), indicating that Tbx20 is not sufficient to induce Tbx2 in the neural tube. These findings suggest that Phox2a/b are upstream regulators of T-box transcription factors in cranial motor neurons, and that Tbx20 and Tbx2 have a different regulatory relationship in neurons compared with that in heart cells (Cai et al., 2005).

Next we screened for changes in the expression of a battery of genes implicated in facial motor neuron development, migration and axon navigation to better understand the molecular basis for the migration defects in *Tbx20* mutants. We focused on BM facial neurons originating from r4 because numerous studies have identified genes required for their migration (reviewed by Chandrasekhar, 2004). In *Tbx20* mutants, we observed ectopic expression of *Ret* in r4 facial neurons, whereas *Ret* is expressed by wild-type facial cells after they migrate caudally from r4 (Fig. 8A-F). However, facial neurons migrated normally in *Ret* mutants (see Fig. S4 in the supplementary material), indicating that this gene is dispensable. Thus, the ectopic expression of *Ret* in *Tbx20* mutants is likely to occur because facial motor neuron cell bodies are unable to depart from r4 in *Tbx20* mutants but they still initiate their normal expression of Ret despite their ectopic location. Similarly, we also detected ectopic expression of neogenin (*Neo1*) within r4 of *Tbx20* mutants, probably due to the stalled migration of facial cells. In the case of genes whose expression normally begins prior to facial cell migration, including *Cdk5*, *Ebf1*, *Unc5h3* (*Unc5c* – Mouse Genome Informatics), neuropilin 1 and neuropilin 2, their expression was maintained within the ectopic r4 motor neurons of *Tbx20* mutants (Fig. 8Y; data not shown). Our results suggest that Tbx20 is dispensable for the expression of these genes, and that these proteins are insufficient to promote the tangential migration of facial neurons in the absence of Tbx20.

Previous studies from zebrafish suggest that PCP signaling components *prickle1* and *tri*/*stbm*/*vang2* are required for facial neuron migration (Bingham et al., 2002; Carreira-Barbosa et al., 2003; Jessen et al., 2002). This prompted us to examine whether PCP genes are regulated by Tbx20 in facial neurons; these included *Wnt4*, *Wnt5a*, *Wnt11*, *Fzd7*, *Prickle1*, *Prickle2*, *Celsr3/flamingo*, *Vang1* (*Vangl1* – Mouse Genome Informatics), *Vang2*/*Stbm*/*Tri* (*Vangl2* – Mouse Genome Informatics), dishevelled (*Dsh1*), dishevelled 2 (*Dsh2*) and dishevelled 3 (*Dsh3*) (*Dvl1*, *Dvl2* and *Dvl3*, respectively – Mouse Genome Informatics) (Fig. 8G-Y, and data not shown). Among the genes examined, *Wnt11*, *Fzd7*, *Pk1*, *Vang1*, *Vang2*, *Celsr3* and *Dsh3* were detected in wild-type facial cells as they migrated from r4 to r6. We found that *Wnt11*, *Fzd7*, *Vang1* and *Vang2* were significantly downregulated and *Pk1* was moderately reduced in facial neurons located within r4 of *Tbx20* mutants. *Dsh3* and *Celsr3* were more broadly expressed in many neural tube cells, including facial neurons, and were unaffected by the loss of Tbx20 (Fig. 8G-Y, and see Fig. S6 in the supplementary material). We also observed a loss of cadherin 8 expression (Fig. 8Y); however, we cannot exclude the possibility that this is an indirect consequence of facial neurons being trapped in r4 as cadherin 8 is normally only expressed after cells enter into r6 (Garel et al., 2000). Our results reveal that Tbx20 is required for the coordinate expression of multiple components of the PCP pathway within migrating facial neurons.

## DISCUSSION

Here we demonstrated that Tbx20 is selectively expressed by two major populations of cranial motor neurons: BM and VM cells. Unlike SM neurons, BM/VM neurons migrate extensively within the hindbrain after they are generated. Using a conditional allele of *Tbx20*, we found that BM/VM neurons in the mouse develop without Tbx20, but their subsequent cell body movements failed to occur. Trigeminal BM and facial VM neurons were unable to migrate dorsolaterally, facial BM neurons did not migrate tangentially, and vestibuloacoustic neurons failed to migrate across the midline. Our study unmasks a shared genetic link used by diverse populations of migratory motor neurons in the hindbrain.

### Hierarchy of transcription factors for branchiomotor and visceromotor neuron development

During BM/VM neuron development the serial actions of multiple transcription factors are believed to build a hierarchal cascade that ensures the proper cell specification and subsequent differentiation of motor neuron subtypes (reviewed by Chandrasekhar, 2004). Naturally, the roles of these transcription factors and the degree of defects that arise in their absence vary. *Phox2b* is essential for assigning BM/VM neuronal fates and consequently mutations in this gene result in the loss of the entire BM/VM cell population (Pattyn et al., 2000). In the absence of *Mash1* and *Math3*, which are restricted to the progenitors of BM/VM cells, hindbrain motor neurons are generated but their identity is mis-specified and therefore later features of their maturation, such as cell body migration, fail to occur properly (Ohsawa et al., 2005). By contrast, the elimination of *Nkx6.1*, whose expression extends into the post-mitotic BM/VM neurons, does not appear to switch motor neuron subtype identity but is needed to regulate their migration (Muller et al., 2003). Thus, depending on the timing and location of expression, each factor performs specific roles in controlling BM/VM neuron development.

In which step does Tbx20 participate in this hierarchy? Our study illustrates that Tbx20 is selectively expressed in BM/VM neurons after their post-mitotic generation. Given that motor neuron identity is thought to be specified prior to the expression of Tbx20 (Briscoe and Ericson, 2001; Jessell, 2000), it is not unexpected that this factor is dispensable for the generation of these neurons. We found that BM/VM cells are generated, survive, extend axons and appropriately express a wide array of genes in *Tbx20* mutants. Importantly, the overall transcription factor profile of these neurons was intact. These findings indicate that the identity of BM/VM cells is properly established independently of Tbx20 function. However, we did find that *Tbx2* expression was downregulated in *Tbx20* mutants. Since Phox2a induced *Tbx20* and *Tbx2* expression, we propose that Tbx20 and Tbx2 are relatively late post-mitotic end products of the genetic cascade controlling BM/VM neuron development (Fig. 8Z).

Our findings differ somewhat from those reported by Takeuchi et al. using RNA interference to knock down Tbx20 expression (Takeuchi et al., 2005). These authors report that Isl2 and Hb9 are downregulated following interference of Tbx20 expression. However, we did not detect Tbx20 expression in the motor neuron subtypes that express Isl2 and/or Hb9 (SM cells) at either hindbrain or spinal cord levels (Fig. 1, and data not shown), nor did we find a

change in the expression of these markers in our mutants. Likewise, the phenotype in the heart of *Tbx20*-null mutants differs from that described using RNA interference (Cai et al., 2005; Singh et al., 2005; Stennard et al., 2005; Takeuchi et al., 2005). The basis for these differences remains to be determined, but might have arisen from non-specific RNAi effects or a general delay in development reported with the embryos (Takeuchi et al., 2005).

### Tbx20 regulates cell body migration of trigeminal, facial and vestibuloacoustic neurons

Neuronal migration is observed in many regions of the brain and is thought to facilitate the formation of more complex circuits comprising multiple neuronal types (Hatten, 1999; Marin and Rubenstein, 2003). Thus, a variety of human disorders have been identified that arise due to neuronal migration defects, including lissencephaly and Kallmann syndrome (reviewed by Gleeson, 2001). Numerous signaling molecules and cytoskeletal proteins have been identified that are crucial for neuronal migration and it has long been appreciated that neuronal interactions with glial cells represent one of the mechanisms that guides the migration process (reviewed by Bielas et al., 2004; Hatten, 1999). The most striking defect found in *Tbx20* mutants was a lack of BM/VM cell migration. Although these two motor neuron classes are functionally related, they comprise diverse motor neuron subtypes that undergo different patterns of cell soma migration. Facial BM neurons migrate tangentially from r4 into r6 orthogonal to the radial glial fibers, whereas trigeminal BM neurons in r2 migrate dorsolaterally along a non-radial pathway. Vestibuloacoustic cells display a third type of cell body movement, migrating across the midline at r4 to the contralateral side of the hindbrain (Chandrasekhar, 2004; Fritzsch et al., 1993; Simon and Lumsden, 1993). The last step in the migration of these motor neuron subtypes is shared, comprising the radial migration of the cell bodies toward their final settling position near the pial surface of the neural tube.

Genetic studies of facial motor neuron migration have found that separate signaling pathways are involved in the initial tangential and later radial migration of these cells (Garel et al., 2000; Muller et al., 2003; Rossel et al., 2005; Schwarz et al., 2004). Despite defects in tangential migration in *VEGF164* mutants, the radial migration of facial cells is preserved, suggesting that other signals are responsible for this migratory process (Schwarz et al., 2004). Accordingly, *Reeler* mutant mice, lacking the reelin extracellular matrix protein, exhibit defects in the radial pattern of BM/VM cell movement, but the tangential path of soma migration is intact (Rossel et al., 2005). Our analysis did not focus on the late phase of radial migration because the earlier steps in motor neuron migration were found to be defective, making it unclear whether radial migration depends on Tbx20. Despite the expectation that each migration pathway will rely on different signaling, we found that all BM/VM neurons share a common requirement for Tbx20. This finding makes it less likely that Tbx20 is alone sufficient to specify the directionality of neuronal migration in response to extrinsic cues. Consistent with this, we did not observe changes in the expression of cell surface molecules, such as neuropilin 1 and neuropilin 2, implicated in controlling the tangential migration of facial BM neurons (Fig. 8) (Schwarz et al., 2004). Although it is possible that Tbx20 controls the expression of components that comprise the general machinery required for neuronal migration, this seems unlikely for several reasons. First, we did not observe a change in expression of components of the general machinery for cell

migration such as Cdk5 (Fig. 8) (Ohshima et al., 2002). Second, Tbx20 is not expressed by all migrating neuronal populations, but is restricted to BM/VM cells. Third, the overall ability to extend axons appeared normal in motor neurons lacking Tbx20, arguing against a major cytoskeletal defect.

In principle, we would predict that the mis-expression of Tbx20 in SM neurons in the hindbrain might lead to ectopic cell body migration. We attempted to test this by electroporating Tbx20 expression constructs into the neural tube of chick embryos; however, we found that this triggered the ectopic formation of motor neurons (see Fig. S5 in the supplementary material). This activity made it difficult to assess whether motor neurons residing in ectopic locations had differentiated at this site or migrated there following the mis-expression of Tbx20. We did not expect Tbx20 to be sufficient to promote motor neuron differentiation in chick embryos because our loss-of-function analysis demonstrated that Tbx20 is not required to generate motor neurons in mice. We discovered that Tbx20 mis-expression induces HNF3$\beta^+$ floor plate cells (see Fig. S5 in the supplementary material). Since the floor plate is a source of sonic hedgehog for motor neuron differentiation (Jessell, 2000), it is possible that the ectopic appearance of motor neurons following Tbx20 mis-expression occurs through a non-cell-autonomous pathway. The basis for this neomorphic activity of ectopically-expressed Tbx20 is unknown, but might reflect the ability of Tbx20 to mimic the activity of other Tbx factors, such as brachyury, in the notochord (Wilkinson et al., 1990).

### Tbx20 controls planar cell polarity signaling in facial neurons

Our search to find downstream targets of Tbx20 led to the identification of components of the PCP pathway: Wnt11 is a ligand; Fzd7 is a receptor; Vang1, Vang2 and Celsr3 are cell surface molecules; and Pk1 and Dsh are intracellular molecules (Montcouquiol et al., 2006; Saburi and McNeill, 2005). Among these, zebrafish mutants lacking *stbm*/*tri*/*vang2* and *pk1* have facial cell migration defects (Bingham et al., 2002; Carreira-Barbosa et al., 2003; Jessen et al., 2002). We observed downregulation of multiple components of the PCP pathway including *Stbm*/*Tri*/*Vang2* and *Pk1*, providing compelling evidence that Tbx20 controls facial cell migration by regulating PCP signaling in these cells (Fig. 8Z). Studies from zebrafish have found evidence for both cell-autonomous and non-autonomous functions of PCP components in mediating facial cell migration (Bingham et al., 2002; Carreira-Barbosa et al., 2003; Jessen et al., 2002). Thus, it is somewhat surprising to find that a motor neuron-specific regulator such as Tbx20 is required to target PCP gene expression specifically to facial motor neurons. This might be interpreted to suggest that PCP genes function cell autonomously within mammalian facial motor neurons. Nevertheless, we found that Vang2 is normally expressed in a heterogeneous salt-and-pepper pattern among migrating facial motor neurons, consistent with it having non-autonomous functions. Although further studies are needed to confirm this, PCP signaling might occur between neighboring motor neurons such that cells that form the facial motor nucleus might influence the migration of one another.

Despite the strong correlation between Tbx20 and the PCP pathway in facial cells, we did not observe the presence of PCP components in trigeminal and vestibuloacoustic motor

neurons. Thus, the transcriptional activity of Tbx20 appears to be highly context-dependent, and capable of controlling different cell migration programs in a cell type-specific manner. In facial motor neurons, Tbx20 regulates the caudally-directed migration of cells via control over the PCP pathway, whereas in trigeminal and vestibuloacoustic cells Tbx20 regulates cell migration by a different means.

## Supplementary Material

Refer to Web version on PubMed Central for supplementary material.

## Acknowledgments

We thank Y. Kawakami for providing chick *Tbx2* and T. T. Kroll for providing *Mash1*, J. F. Brunet for providing Phox2b antibody and *Phox2a* cDNA, and the Beta Cell Biology Consortium for antibodies. We thank J. E. Rivier and J. M. Vaughan for their help in generating Tbx20 antibodies, J. W. Lewcock for *SE1::gfp* transgenic mice and F. Costantini for *Ret* mutant mice. We thank A. Ghosh for comments on the manuscript. We are grateful to members of the S.L.P. laboratory for helpful discussions and encouragement, and to K. Lettieri and A. Bryson for technical assistance. M.-R.S. was supported by a fellowship from the Paralyzed Veterans Association; S.-K.L. by a fellowship from the Human Frontiers Program; R.S. by fellowships from the Pioneer Foundation and the Maximilian & Marion Hoffman Foundation; C.-L.C. by an AHA National Scientist Development Grant; and S.M.E. by NIH 1RO1 HL070867. This research was funded by grants from the NINDS and Project ALS to S.L.P.

## References

Ahn DG, Ruvinsky I, Oates AC, Silver LM, Ho RK. tbx20, a new vertebrate T-box gene expressed in the cranial motor neurons and developing cardiovascular structures in zebrafish. Mech Dev. 2000; 95:253–258. [PubMed: 10906473]

Bell E, Lumsden A, Graham A. Expression of GATA-2 in the developing avian rhombencephalon. Mech Dev. 1999a; 84:173–176. [PubMed: 10473136]

Bell E, Wingate RJ, Lumsden A. Homeotic transformation of rhombomere identity after localized Hoxb1 misexpression. Science. 1999b; 284:2168–2171. [PubMed: 10381880]

Bielas S, Higginbotham H, Koizumi H, Tanaka T, Gleeson JG. Cortical neuronal migration mutants suggest separate but intersecting pathways. Annu Rev Cell Dev Biol. 2004; 20:593–618. [PubMed: 15473853]

Bingham S, Higashijima S, Okamoto H, Chandrasekhar A. The Zebrafish trilobite gene is essential for tangential migration of branchiomotor neurons. Dev Biol. 2002; 242:149–160. [PubMed: 11820812]

Briscoe J, Ericson J. Specification of neuronal fates in the ventral neural tube. Curr Opin Neurobiol. 2001; 11:43–49. [PubMed: 11179871]

Cai CL, Zhou W, Yang L, Bu L, Qyang Y, Zhang X, Li X, Rosenfeld MG, Chen J, Evans S. T-box genes coordinate regional rates of proliferation and regional specification during cardiogenesis. Development. 2005; 132:2475–2487. [PubMed: 15843407]

Carreira-Barbosa F, Concha ML, Takeuchi M, Ueno N, Wilson SW, Tada M. Prickle 1 regulates cell movements during gastrulation and neuronal migration in zebrafish. Development. 2003; 130:4037–4046. [PubMed: 12874125]

Chandrasekhar A. Turning heads: development of vertebrate branchiomotor neurons. Dev Dyn. 2004; 229:143–161. [PubMed: 14699587]

Dubreuil V, Hirsch MR, Pattyn A, Brunet JF, Goridis C. The Phox2b transcription factor coordinately regulates neuronal cell cycle exit and identity. Development. 2000; 127:5191–5201. [PubMed: 11060244]

Ericson J, Thor S, Edlund T, Jessell TM, Yamada T. Early stages of motor neuron differentiation revealed by expression of homeobox gene Islet-1. Science. 1992; 256:1555–1560. [PubMed: 1350865]

Fink AJ, Englund C, Daza RA, Pham D, Lau C, Nivison M, Kowalczyk T, Hevner RF. Development of the deep cerebellar nuclei: transcription factors and cell migration from the rhombic lip. J Neurosci. 2006; 26:3066–3076. [PubMed: 16540585]

Fong SH, Emelyanov A, Teh C, Korzh V. Wnt signalling mediated by Tbx2b regulates cell migration during formation of the neural plate. Development. 2005; 132:3587–3596. [PubMed: 16033799]

Fritzsch B. Development of the labyrinthine efferent system. Ann New York Acad Sci. 1996; 781:21–33. [PubMed: 8694416]

Fritzsch B, Christensen MA, Nichols DH. Fiber pathways and positional changes in efferent perikarya of 2.5- to 7-day chick embryos as revealed with DiI and dextran amines. J Neurobiol. 1993; 24:1481–1499. [PubMed: 7506749]

Garel S, Garcia-Dominguez M, Charnay P. Control of the migratory pathway of facial branchiomotor neurones. Development. 2000; 127:5297–5307. [PubMed: 11076752]

Gleeson JG. Neuronal migration disorders. Ment Retard Dev Disabil Res Rev. 2001; 7:167–171. [PubMed: 11553932]

Goddard JM, Rossel M, Manley NR, Capecchi MR. Mice with targeted disruption of Hoxb-1 fail to form the motor nucleus of the VIIth nerve. Development. 1996; 122:3217–3228. [PubMed: 8898234]

Hatcher CJ, Diman NY, Kim MS, Pennisi D, Song Y, Goldstein MM, Mikawa T, Basson CT. A role for Tbx5 in proepicardial cell migration during cardiogenesis. Physiol Genomics. 2004; 18:129–140. [PubMed: 15138308]

Hatten ME. Central nervous system neuronal migration. Annu Rev Neurosci. 1999; 22:511–539. [PubMed: 10202547]

Jessell TM. Neuronal specification in the spinal cord: inductive signals and transcriptional codes. Nat Rev Genet. 2000; 1:20–29. [PubMed: 11262869]

Jessen JR, Topczewski J, Bingham S, Sepich DS, Marlow F, Chandrasekhar A, Solnica-Krezel L. Zebrafish trilobite identifies new roles for Strabismus in gastrulation and neuronal movements. Nat Cell Biol. 2002; 4:610–615. [PubMed: 12105418]

Kraus F, Haenig B, Kispert A. Cloning and expression analysis of the mouse T-box gene tbx20. Mech Dev. 2001; 100:87–91. [PubMed: 11118890]

Manzanares M, Trainor PA, Nonchev S, Ariza-McNaughton L, Brodie J, Gould A, Marshall H, Morrison A, Kwan CT, Sham MH, et al. The role of kreisler in segmentation during hindbrain development. Dev Biol. 1999; 211:220–237. [PubMed: 10395784]

Marin O, Rubenstein JL. Cell migration in the forebrain. Annu Rev Neurosci. 2003; 26:441–483. [PubMed: 12626695]

Montcouquiol M, Crenshaw EB, Kelley MW. Noncanonical Wnt signaling and neural polarity (1). Annu Rev Neurosci. 2006; 29:363–386. [PubMed: 16776590]

Moraes F, Novoa A, Jerome-Majewska LA, Papaioannou VE, Mallo M. Tbx1 is required for proper neural crest migration and to stabilize spatial patterns during middle and inner ear development. Mech Dev. 2005; 122:199–212. [PubMed: 15652707]

Muller M, Jabs N, Lorke DE, Fritzsch B, Sander M. Nkx6.1 controls migration and axon pathfinding of cranial branchio-motoneurons. Development. 2003; 130:5815–5826. [PubMed: 14534138]

Naiche LA, Harrelson Z, Kelly RG, Papaioannou VE. T-box genes in vertebrate development. Annu Rev Genet. 2005; 39:219–239. [PubMed: 16285859]

Nakamura H, Watanabe Y, Funahashi J. Misexpression of genes in brain vesicles by in ovo electroporation. Dev Growth Differ. 2000; 42:199–201. [PubMed: 10910124]

Nardelli J, Thiesson D, Fujiwara Y, Tsai FY, Orkin SH. Expression and genetic interaction of transcription factors GATA-2 and GATA-3 during development of the mouse central nervous system. Dev Biol. 1999; 210:305–321. [PubMed: 10357893]

Ohsawa R, Ohtsuka T, Kageyama R. Mash1 and Math3 are required for development of branchiomotor neurons and maintenance of neural progenitors. J Neurosci. 2005; 25:5857–5865. [PubMed: 15976074]

Ohshima T, Ogawa M, Takeuchi K, Takahashi S, Kulkarni AB, Mikoshiba K. Cyclin-dependent kinase 5/p35 contributes synergistically with Reelin/Dab1 to the positioning of facial branchiomotor and

inferior olive neurons in the developing mouse hindbrain. J Neurosci. 2002; 22:4036–4044. [PubMed: 12019323]

Pata I, Studer M, van Doorninck JH, Briscoe J, Kuuse S, Engel JD, Grosveld F, Karis A. The transcription factor GATA3 is a downstream effector of Hoxb1 specification in rhombomere 4. Development. 1999; 126:5523–5531. [PubMed: 10556076]

Pattyn A, Hirsch M, Goridis C, Brunet JF. Control of hindbrain motor neuron differentiation by the homeobox gene Phox2b. Development. 2000; 127:1349–1358. [PubMed: 10704382]

Rossel M, Loulier K, Feuillet C, Alonso S, Carroll P. Reelin signaling is necessary for a specific step in the migration of hindbrain efferent neurons. Development. 2005; 132:1175–1185. [PubMed: 15703280]

Saburi S, McNeill H. Organising cells into tissues: new roles for cell adhesion molecules in planar cell polarity. Curr Opin Cell Biol. 2005; 17:482–488. [PubMed: 16099635]

Schneider-Maunoury S, Topilko P, Seitandou T, Levi G, Cohen-Tannoudji M, Pournin S, Babinet C, Charnay P. Disruption of Krox-20 results in alteration of rhombomeres 3 and 5 in the developing hindbrain. Cell. 1993; 75:1199–1214. [PubMed: 7903221]

Schneider-Maunoury S, Seitanidou T, Charnay P, Lumsden A. Segmental and neuronal architecture of the hindbrain of Krox-20 mouse mutants. Development. 1997; 124:1215–1226. [PubMed: 9102308]

Schuchardt A, D'Agati V, Larsson-Blomberg L, Costantini F, Pachnis V. Defects in the kidney and enteric nervous system of mice lacking the tyrosine kinase receptor Ret. Nature. 1994; 367:380–383. [PubMed: 8114940]

Schwarz Q, Gu C, Fujisawa H, Sabelko K, Gertsenstein M, Nagy A, Taniguchi M, Kolodkin AL, Ginty DD, Shima DT, et al. Vascular endothelial growth factor controls neuronal migration and cooperates with Sema3A to pattern distinct compartments of the facial nerve. Genes Dev. 2004; 18:2822–2834. [PubMed: 15545635]

Seitanidou T, Schneider-Maunoury S, Desmarquet C, Wilkinson DG, Charnay P. Krox-20 is a key regulator of rhombomere-specific gene expression in the developing hindbrain. Mech Dev. 1997; 65:31–42. [PubMed: 9256343]

Sharma K, Sheng HZ, Lettieri K, Li H, Karavanov A, Potter S, Westphal H, Pfaff SL. LIM homeodomain factors Lhx3 and Lhx4 assign subtype identities for motor neurons. Cell. 1998; 95:817–828. [PubMed: 9865699]

Shirasaki R, Tamada A, Katsumata R, Murakami F. Guidance of cerebellofugal axons in the rat embryo: directed growth toward the floor plate and subsequent elongation along the longitudinal axis. Neuron. 1995; 14:961–972. [PubMed: 7748563]

Shirasaki R, Katsumata R, Murakami F. Change in chemoattractant responsiveness of developing axons at an intermediate target. Science. 1998; 279:105–107. [PubMed: 9417018]

Shirasaki R, Lewcock JW, Lettieri K, Pfaff SL. FGF as a target-derived chemoattractant for developing motor axons genetically programmed by the LIM code. Neuron. 2006; 50:841–853. [PubMed: 16772167]

Simon H, Lumsden A. Rhombomere-specific origin of the contralateral vestibulo-acoustic efferent neurons and their migration across the embryonic midline. Neuron. 1993; 11:209–220. [PubMed: 8394719]

Singh MK, Christoffels VM, Dias JM, Trowe MO, Petry M, Schuster-Gossler K, Burger A, Ericson J, Kispert A. Tbx20 is essential for cardiac chamber differentiation and repression of Tbx2. Development. 2005; 132:2697–2707. [PubMed: 15901664]

Smith J. T-box genes: what they do and how they do it. Trends Genet. 1999; 15:154–158. [PubMed: 10203826]

Stennard FA, Costa MW, Elliott DA, Rankin S, Haast SJ, Lai D, McDonald LP, Niederreither K, Dolle P, Bruneau BG, et al. Cardiac T-box factor Tbx20 directly interacts with Nkx2-5, GATA4, and GATA5 in regulation of gene expression in the developing heart. Dev Biol. 2003; 262:206–224. [PubMed: 14550786]

Stennard FA, Costa MW, Lai D, Biben C, Furtado MB, Solloway MJ, McCulley DJ, Leimena C, Preis JI, Dunwoodie SL, et al. Murine T-box transcription factor Tbx20 acts as a repressor during heart

development, and is essential for adult heart integrity, function and adaptation. Development. 2005; 132:2451–2462. [PubMed: 15843414]

Studer M. Initiation of facial motoneurone migration is dependent on rhombomeres 5 and 6. Development. 2001; 128:3707–3716. [PubMed: 11585797]

Studer M, Lumsden A, Ariza-McNaughton L, Bradley A, Krumlauf R. Altered segmental identity and abnormal migration of motor neurons in mice lacking Hoxb-1. Nature. 1996; 384:630–634. [PubMed: 8967950]

Swiatek PJ, Gridley T. Perinatal lethality and defects in hindbrain development in mice homozygous for a targeted mutation of the zinc finger gene Krox20. Genes Dev. 1993; 7:2071–2084. [PubMed: 8224839]

Takeuchi JK, Mileikovskaia M, Koshiba-Takeuchi K, Heidt AB, Mori AD, Arruda EP, Gertsenstein M, Georges R, Davidson L, Mo R, et al. Tbx20 dose-dependently regulates transcription factor networks required for mouse heart and motoneuron development. Development. 2005; 132:2463–2474. [PubMed: 15843409]

Tanabe Y, William C, Jessell TM. Specification of motor neuron identity by the MNR2 homeodomain protein. Cell. 1998; 95:67–80. [PubMed: 9778248]

Thaler J, Harrison K, Sharma K, Lettieri K, Kehrl J, Pfaff SL. Active suppression of interneuron programs within developing motor neurons revealed by analysis of homeodomain factor HB9. Neuron. 1999; 23:675–687. [PubMed: 10482235]

Thaler JP, Koo SJ, Kania A, Lettieri K, Andrews S, Cox C, Jessell TM, Pfaff SL. A postmitotic role for Isl-class LIM homeodomain proteins in the assignment of visceral spinal motor neuron identity. Neuron. 2004; 41:337–350. [PubMed: 14766174]

Tiveron MC, Pattyn A, Hirsch MR, Brunet JF. Role of Phox2b and Mash1 in the generation of the vestibular efferent nucleus. Dev Biol. 2003; 260:46–57. [PubMed: 12885554]

Uemura O, Okada Y, Ando H, Guedj M, Higashijima S, Shimazaki T, Chino N, Okano H, Okamoto H. Comparative functional genomics revealed conservation and diversification of three enhancers of the isl1 gene for motor and sensory neuron-specific expression. Dev Biol. 2005; 278:587–606. [PubMed: 15680372]

Wilkinson DG, Bhatt S, Herrmann BG. Expression pattern of the mouse T gene and its role in mesoderm formation. Nature. 1990; 343:657–659. [PubMed: 1689462]

Yamamoto N, Kurotani T, Toyama K. Neural connections between the lateral geniculate nucleus and visual cortex in vitro. Science. 1989; 245:192–194. [PubMed: 2749258]

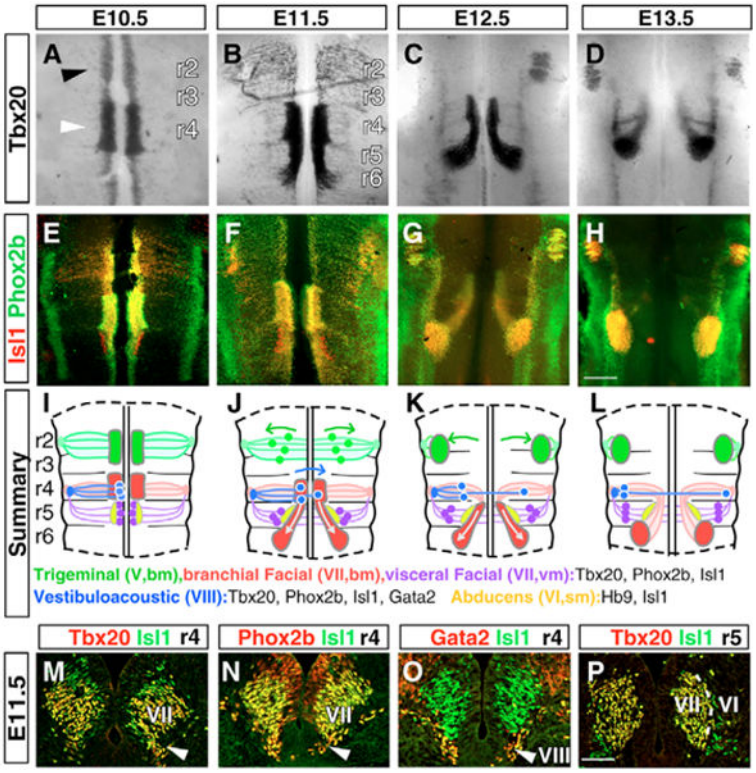


**Fig. 1. *Tbx20* is expressed by branchiomotor and visceromotor neurons**

(**A-D**) In situ hybridization analysis of *Tbx20* expression in flat-mounted hindbrains between E10.5 and E13.5. *Tbx20* is expressed in ventral columns of motor neurons flanking the midline at E10.5 (A). Trigeminal neurons are labeled at r2 (black arrowhead) and facial neurons at r4 (white arrowhead). (**E-H**) Isl1 (red) and Phox2b (green) co-expression (yellow) defines the location of BM and VM neurons in flat-mounted hindbrains. The expression of *Tbx20* mirrors the pattern of Isl1 and Phox2b double-labeling. (**I-L**) Summary depicting the cell body migration patterns and transcription factor profiles of hindbrain motor neurons. At present, it is unclear whether all or only a subset of vestibuloacoustic neurons (blue) cross the midline. (**M-P**) Immunohistochemistry of E11.5 hindbrain transverse sections. Facial neurons co-express Isl1, Tbx20 and Phox2b. Vestibuloacoustic neurons (white arrowhead) express Gata2 and Isl1. (P) Abducens (VI) SM neurons at r5 lack Tbx20; the dashed line indicates the border between facial (VII) and abducens (VI) neurons. Scale bars: in H, 500 μm for A-H; in P, 50 μm for M-P.

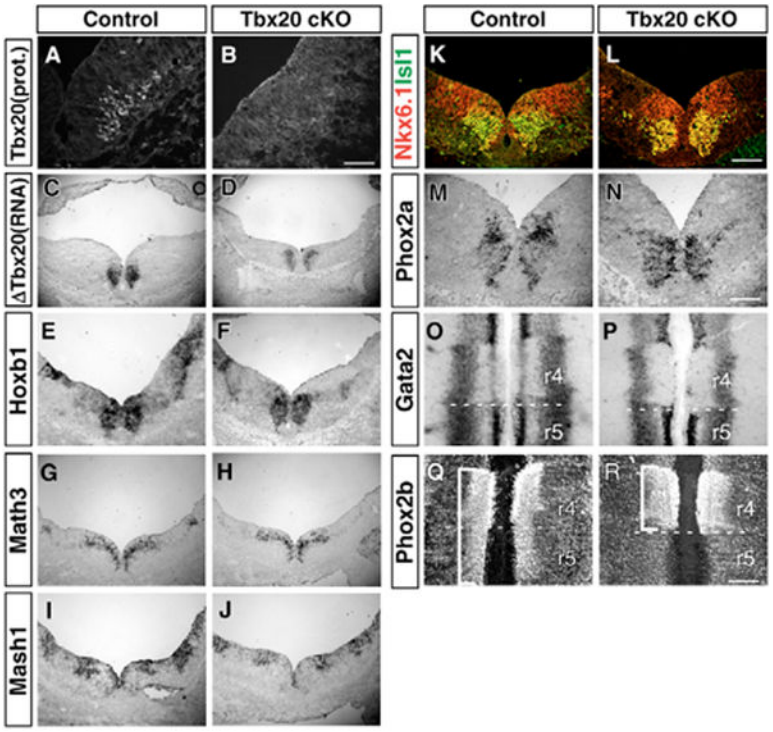


**Fig. 2. Facial motor neuron specification is normal in *Tbx20* conditional mutants**

Gene expression profile analysis in transverse sections at r4 (**A-N**) or flat-mounted hindbrains (**O-R**). (A,B) *Tbx20* cKO mutant mice lack Tbx20 protein in the neural tube. (C,D) *Tbx20*-null cells are viable and detected by their expression of the non-functional *Tbx20* transcript. (E-N) *Hoxb1*, *Math3*, *Mash1*, Isl1, Nkx6.1 and *Phox2a* are expressed normally in *Tbx20* mutants. (O,P) *Gata2* expression is normal in *Tbx20* mutants, although medial GATA2 labeling in r4 is reduced (dashed line marks the r4/r5 border). (Q,R) Phox2b expression (bracketed) is confined to r4 in *Tbx20* mutants, whereas controls exhibit labeling in r4 and r5. The altered Phox2b labeling pattern indicates a cell migration defect. Data are representative of at least twelve sections from at least three embryos of each genotype. Scale bars: in B, 40 μm for A,B; in L, 80 μm for C-L; in N, 160 μm for M,N; in R, 300 μm for O-R.

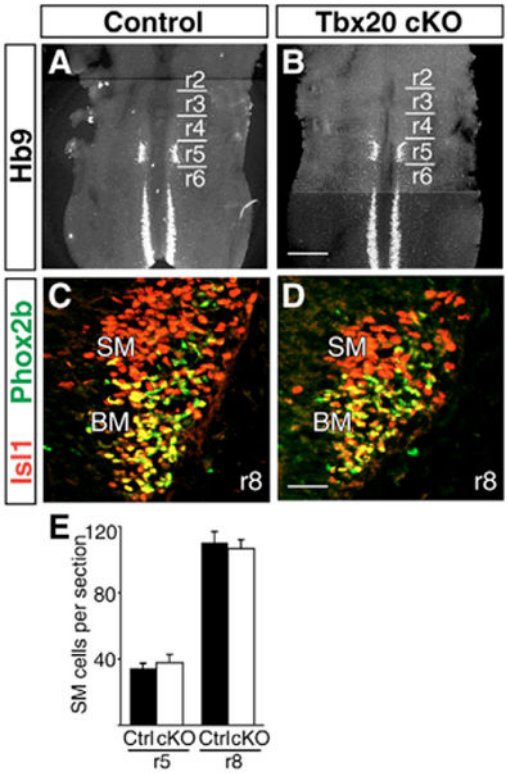


**Fig. 3. BM/VM cells lacking Tbx20 do not convert their fate into somatic motor neurons**

(**A**,**B**) The SM neuron marker Hb9 is expressed normally in E11.5 flat-mounted hindbrains from *Tbx20* cKOs. (**C**,**D**) Isl1 (red) and Phox2b (green) expression in r8 transverse sections from E10.5 *Tbx20* mutants and controls. Hypoglossal (XII) SM cells express Isl1 (red) whereas spinal accessory (XI) BM neurons co-express Isl1 and Phox2b (yellow). (**E**) Quantification of the number of SM neurons ($Hb9^+$ or $Isl1^+/Phox2b^-$) in *Tbx20* mutants and controls at r5 (E11.5) and r8 (E10.5). Each bar represents the average of at least eight sections collected from three different embryos; mean±s.e.m. Scale bars: in B, 500 μm for A,B; in D, 30 μm for C,D.

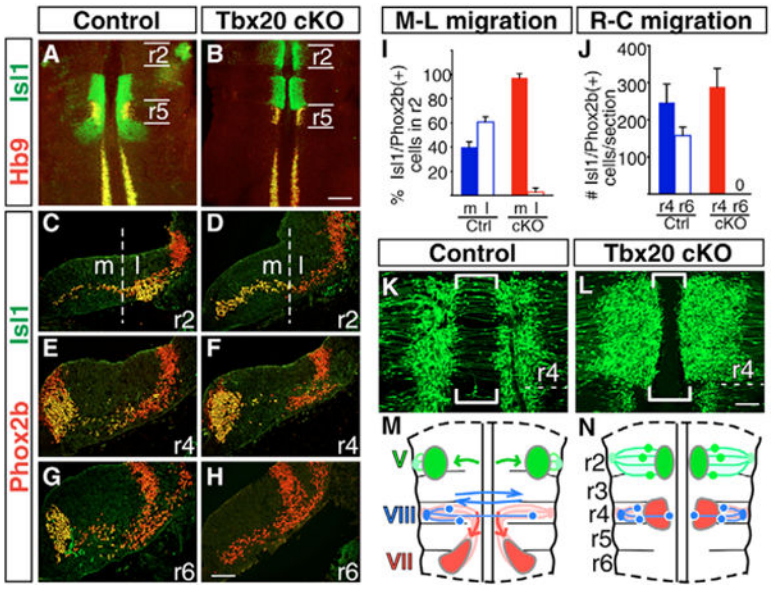


**Fig. 4. Tangential, mediolateral and trans-median defects in cell body migration occur in *Tbx20* mutants**

(**A**,**B**) Isl1 (green) and Hb9 (red) expression in flat-mounted hindbrains from E11.5 *Tbx20* mutant and control. Trigeminal neurons ($Isl1^+/Hb9^-$) at r2 fail to migrate laterally and radially in *Tbx20* mutants. Facial BM neurons ($Isl1^+/Hb9^-$) at r4 do not migrate caudally past the $Isl1^+/Hb9^+$ abducens cells (yellow, r5) in *Tbx20* mutants. (**C-H**) Comparison of Isl1 (green) and Phox2b (red) expression in transverse sections between E11.5 *Tbx20* mutants and controls (in r2, r4 and r6). Dashed line in C,D indicates the border between medial (m) and lateral (l) regions of the hindbrain used for quantification. (**I**) Quantification of mediolateral (M-L) cell movement determined by measuring the ratio of BM neurons ($Isl1^+/Phox2b^+$) located in the medial (m) versus lateral (l) region. Cell counts were performed on transverse sections taken at r2 levels containing trigeminal neurons at E11.5 in *Tbx20* mutants and controls. Each bar represents the average of at least six sections from three different embryos; mean±s.e.m. (**J**) Quantification of rostrocaudal (R-C) migration of facial neurons marked by Isl1/Phox2b double labeling (yellow). Cell counts were taken from transverse sections at r4 and r6 in *Tbx20* mutants and controls. Each bar represents the average of at least eight sections from three different embryos; mean±s.e.m. (**K**,**L**) The *SE1::gfp* transgenic reporter was crossed into the *Tbx20* mutant background to reveal vestibuloacoustic (VIII) motor neuron cell bodies and axons. In E11.5 control embryos, GFP-labeled cells and axons cross the r4 midline (bracket). In *Tbx20* mutants, midline crossing fails to occur. (**M**,**N**) Summary diagram comparing the cell body movements of trigeminal (V), vestibuloacoustic (VIII) and facial (VII) motor neuron migration in *Tbx20* mutants and controls. Images shown are representative of four or more embryos of each genotype. Scale bars: in B, 400 μm for A,B; in H, 80 μm for C-H; in L, 160 μm for K,L.

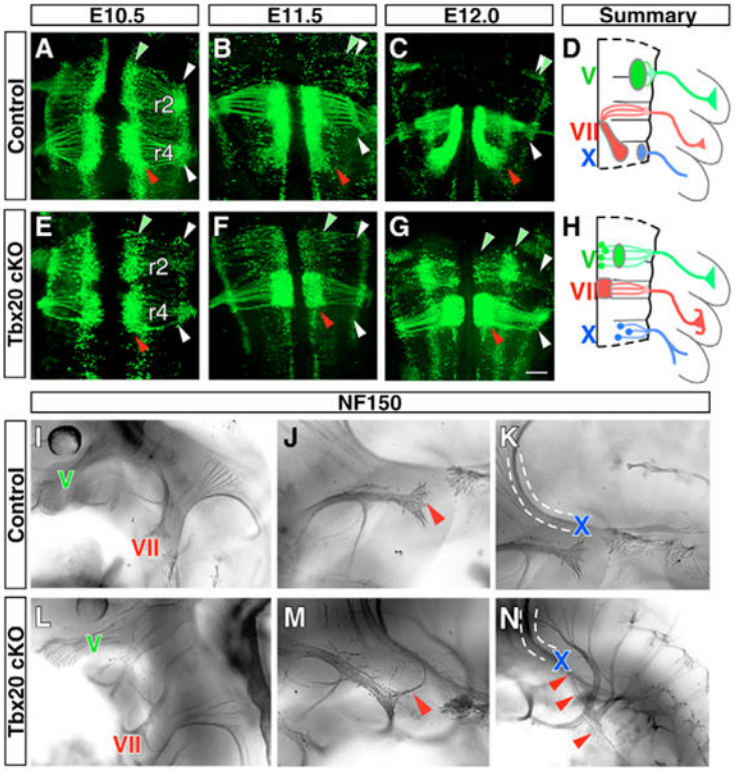


**Fig. 5. BM and VM neurons in *Tbx20* mutants display axon guidance defects**

(**A-H**) Axonal projections in flat-mounted hindbrains of *SE1::gfp*; *Tbx20* mutants and controls. GFP marks BM/VM neurons in *SE1::gfp* transgenic mice (see Fig. S3 in the supplementary material). Axonal exit points of BM/VM neurons (white arrowheads) in hindbrains from *Tbx20* mutants are normal. In *Tbx20* mutants, the cell bodies of trigeminal neurons (green arrowheads in E-G) partially migrate dorsolaterally toward the exit point (white arrowheads), whereas those of facial neurons (red arrowhead in E-G) fail to migrate. These observations are summarized in D and H. (**I-N**) Whole-mount neurofilament staining of axonal projections in E11.5 *Tbx20* mutants and controls. (I,L) Trigeminal axons project toward their correct peripheral targets in *Tbx20* mutants. (J,M) High power view of the embryos shown in I and L revealing abnormal facial axon pathfinding (VII, red arrowhead). (K,N) High power view from I and L at a different focal plane revealing defasciculation and misrouting of vagal (X) axons (red arrowheads); the dashed line indicates the projectory of vagal axons. Scale bar: in G, 500 μm for A-C, E-G.

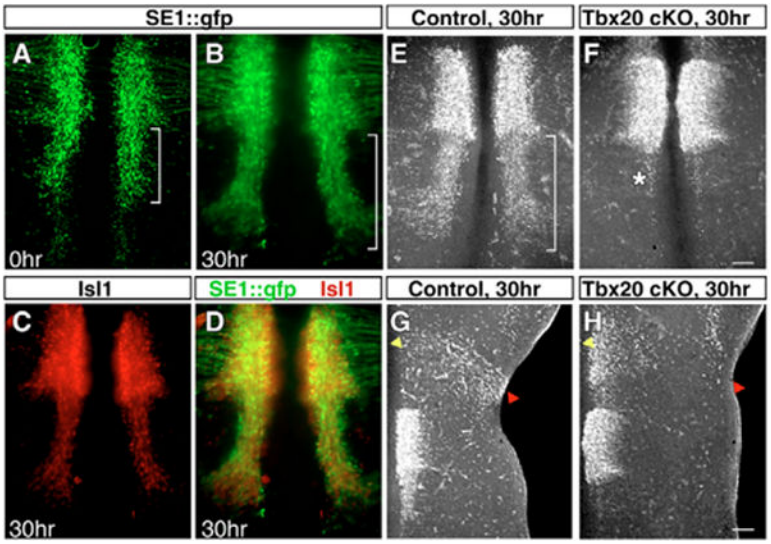


**Fig. 6. Migration defects in *Tbx20* mutants are not due to developmental arrest**

(**A-D**) Flat-mounted hindbrains from E11.5 *SE1::gfp* mice before (A) and after (B-D) organotypic culture. Facial neurons migrate caudally after 30 hours in vitro (compare white brackets in A and B). (**E-H**) Isl1 expression in flat-mounted hindbrain explants from E11.5 *Tbx20* mutants or controls. Facial neurons from *Tbx20* mutants do not migrate, in contrast to the controls. Asterisk in F marks abducens SM neurons at r5. Trigeminal neurons from *Tbx20* mutants fail to migrate laterally; compare medial (yellow arrowhead) and lateral (red arrowhead) $Isl1^+$ cells in *Tbx20* mutants and controls. Scale bars: in F, 250 μm for A-F; in H, 320 μm for G,H.

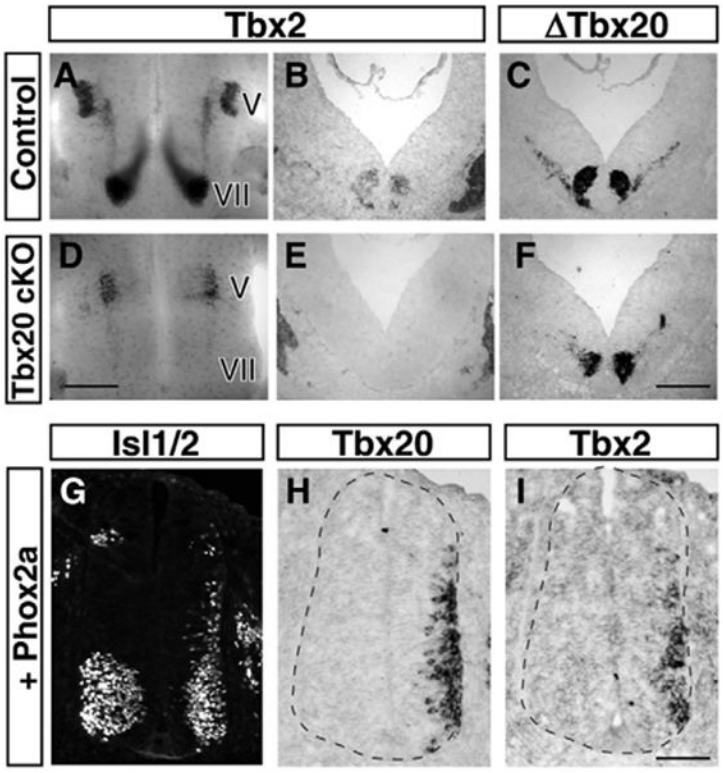


**Fig. 7. A genetic interaction between *Tbx20* and *Tbx2***

(**A-F**) In situ hybridization analysis on flat-mounted hindbrain preparations and transverse sections reveals that *Tbx2* expression is absent in *Tbx20* mutants. The *ΔTbx20* probe detects both full-length and mutated transcripts. Adjacent sections were used to locate *Tbx20*-null cells. (**G-I**) Mis-expression of Phox2a induces *Isl1, Tbx20* and *Tbx2* expression in chick embryonic spinal cord at HH stage 20. Scale bars: in D, 400 μm for A,D; in F, 250 μm for B,C,E,F; in I, 100 μm for G-I.

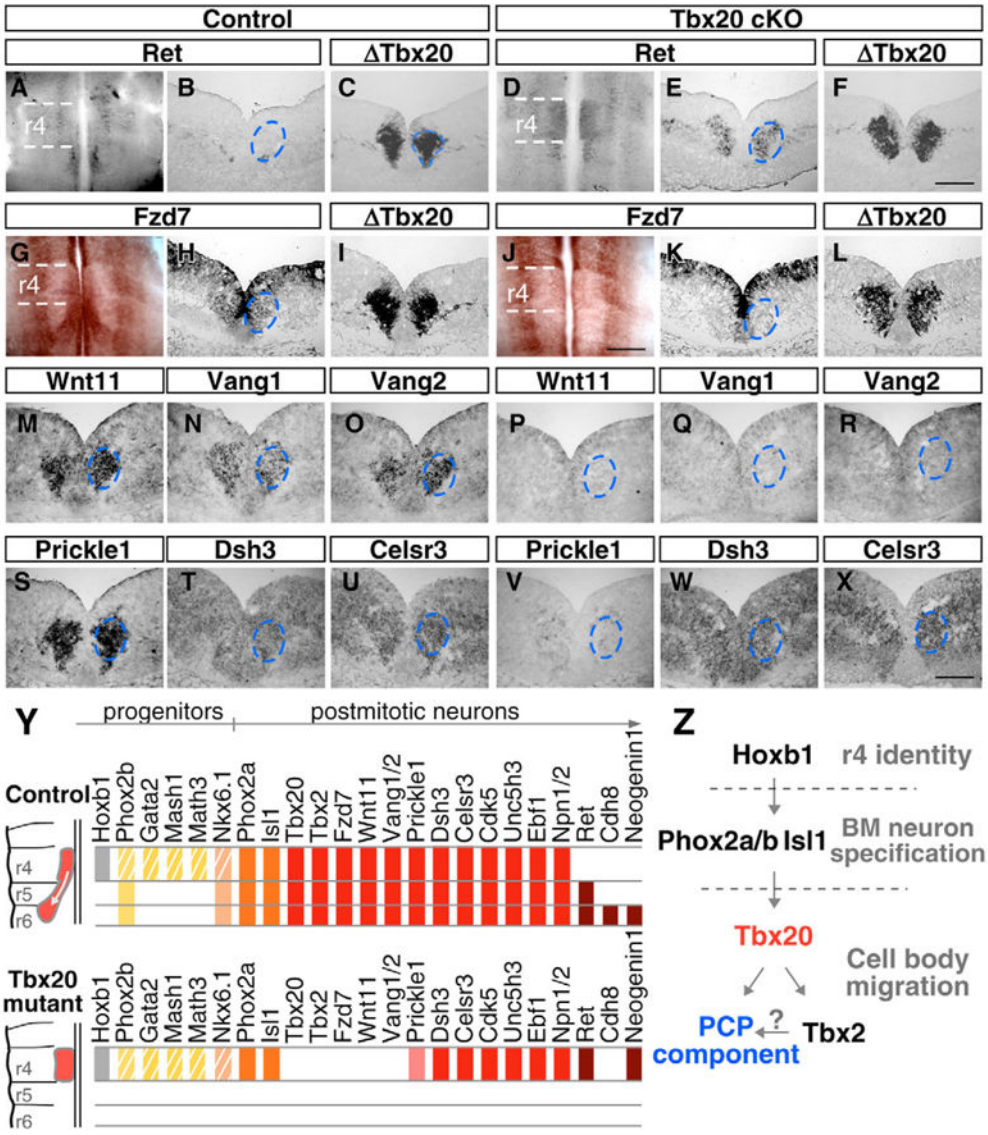


**Fig. 8. PCP pathways are impaired in *Tbx20* mutants**

(**A-X**) *Ret*, *Fzd7, Wnt11, Vang1, Vang2, Pk1, Dsh3* and *Celsr3* expression in flat-mounted hindbrains or transverse sections at r4 from E11.5 *Tbx20* mutants or littermate controls. To localize facial cells at r4, *ΔTbx20* and *Hoxb1* probes were used on adjacent sections (C,F,I,L, and see Fig. S6 in the supplementary material). (A-F) *Ret* is ectopically expressed at r4 in *Tbx20* mutants. (G-R) *Fzd7, Wnt11, Vang1* and *Vang2* are absent at r4 in *Tbx20* mutants, in constrast to controls. (S-X) *Pk1* expression is reduced in *Tbx20* mutants whereas *Dsh3* and *Celsr1* are unchanged. The boundaries of r4 are indicated by the white dashed lines; the blue dashed line encircles facial cells. (**Y**) Summary of genes examined in facial neurons from controls and *Tbx20* mutants. Each bar represents the expression of an individual gene from r4 to r6. Striped bars represent genes expressed by facial neuron progenitors residing at r4. Genes expressed at similar stages are aligned next to each other. (**Z**) Summary of the genetic cascade required (but not necessarily sufficient) for facial motor neuron development and migration based on data presented here and elsewhere (reviewed by

Chandrasekhar, 2004). It is unknown whether Tbx2 is required to activate PCP gene expression. Scale bars: in J, 400 μm for A,D,G,J; in F, 250 μm for B,C,E,F; in X, 110 μm for H,I,K-X.